

05-001

### **EXPERIMENTAL STUDY OF THE OSCILLATING WATER COLUMN TECHNOLOGY ON A WELLS TURBINE.**

Medina López, Encarnación  
Universidad de Granada

Oscillating Water Column (OWC) devices for wave energy extraction are equipped with Wells turbines for energy conversion. The effect of humidity in the air chamber of the OWC entails variations on the atmospheric conditions near the turbine, modifying its performance and efficiency. A theoretical development of a model which includes humidity considerations is done. Moreover, the influence of humid air in the performance of the turbine is studied through experimental tests carried out in a Wind Tunnel seeded with water particles. Results show that power input to the OWC can be reduced in a 40% when humidity in air is taken into account.

**Keywords:** *Oscillating Water Column; OWC; humidity; Real Gas; wave energy; Wells turbine.*

### **ESTUDIO EXPERIMENTAL DE LA COLUMNA DE AGUA OSCILANTE CON APLICACIÓN A LA TURBINA WELLS.**

Los dispositivos de Columna de Agua Oscilante, Oscillating Water Column (OWC), para extracción de energía undimotriz están equipados con turbinas Wells para la conversión de la energía. El efecto de la humedad en el aire de la cámara del OWC conlleva variaciones en las condiciones atmosféricas en el entorno de la turbina, modificando su funcionamiento y eficiencia. A partir del desarrollo de un modelo teórico que incluye consideraciones de humedad y el consecuente estudio experimental llevado a cabo en un Túnel de Viento sembrado con partículas de agua, se estudia la influencia del aire húmedo en el funcionamiento de la turbina. Los resultados muestran que la potencia de entrada al OWC se puede ver reducida en un 40% cuando se tiene en cuenta la humedad del aire.

**Palabras clave:** *Columna de Agua Oscilante; humedad; Gas Real; energía de las olas; undimotriz; turbina Wells.*

Correspondencia: Encarnación Medina López encaramelo@gmail.com

Agradecimientos: A Antonio por sus ideas. A Leo por su apoyo y divergencia. A mis padres y hermana por estar siempre ahí. A mi abuela por creer en mí incondicionalmente.

## 1. INTRODUCTION

Wave energy extraction through OWC devices has been studied during the last decades. The study of this type of system has been analysed on the basis of the analogy with oscillatory rigid bodies, as the OWC consists of a chamber open at the bottom that allows the water surface inside to push the air above through the turbine (Martins-Rivas & Mei, 2009).

Theoretical models have been tested in plants that are currently underway (e.g. Mutriku OWC in Basque Country, or Pico OWC in Azores). The main problem that arises is that the theoretical yields obtained do not match the reality, (Power-technology, 2014).

The OWC model has been developed by various authors. Evans (1982) and Evans & Porter (1995) formulated the problem of the oscillation of the water level in the chamber of OWC by linear wave theory. Sarmento (1990) extended the air expansion-compression problem inside the chamber. Finally, Martins-Rivas & Mei (2009) reported a method of geometric control to maximize the efficiency of power extraction. All these authors start from an adiabatic process considering dry air as an ideal gas. In all previous references prevails the hypothesis of perfect gas –an ideal gas with constant specific volumetric heat- for the compression/expansion process. Consequently, the isentropic law is applied and linearized so the formulation is simplified. In fact, the reference conditions for the OWC are usually fixed as atmospheric, in which dry air is assumed and no further specifications on temperature, density or ambient moisture –dry air and water vapour mixture– are applied. In other words, no real gas model is taken into account.

This is the motivation of this work. Variations in the temperature, ambient moisture and pressure are known to affect the turbine performance. Although the results are usually applied in different fields from that of sea wave energy extraction, the fundamentals of real gases could bring up a new scope in the real working conditions of OWC devices. The changes in performance arise from density diminishing, variations in the specific heat and gas constant, and for the eventual condensation of water vapour. Referring to the study of air temperature effect, moisture and development of models of real gas in gas turbines, there is a lack of knowledge in the State of Art (see for details Singh & Kumar (2012) and Tsonopoulos & Heidman (1990)). The first one (Singh & Kumar, 2012), analyses the effect of ambient air temperature in the net power output on power plant performance. The second one (Tsonopoulos & Heidman, 1990), uses the Virial Theorem to study real gas processes. Even if we establish the fundamental differences between OWC and gas turbine performances, a further step in the formulation of the OWC problem must be considered. We introduce a real gas in the model as well as the influence of ambient conditions, for which a full thermodynamic approach should be taken into account. To fulfil this task, we apply the virial theorem (or the Kammerling—Ones expansion) (see Tsonopoulos & Heidman (1990)). Due to the limitations of the current models, it is desirable a gas model applied to the classical OWC development. This fact would help to understand the response of the OWC system and its relation with the principle of operation under real conditions. As a first approach, this paper studies the fundamentals of turbine operation under changes in density induced by variation of moisture content in steady state.

## 2. AIMS

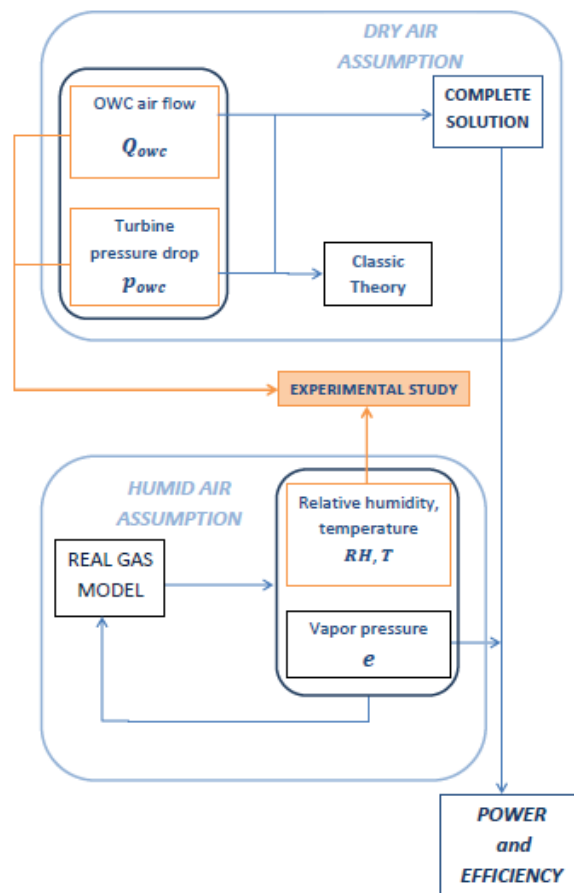
The main goal of this paper is to study the effect of the working fluid density, mainly modified by humidity, on the performance of a Wells turbine on a steady state accounting for the real gas nature. To reach this purpose, some specific aims have to be checked:

- To present the Wells turbine operating problem, considering it as a real gas model (mixture of dry air and water vapour).
- To experimentally verify the effect of moisture on the performance of a Wells turbine.

### 3. METHODOLOGY

To face these objectives, the methodology is essentially based upon experimental determination of pressure jump and flow characteristics in a simplified turbine model, and the theoretical formulation of the thermodynamic problem. The scheme shown in figure 1 describes the work flow to reach the final goals.

**Figure 1: General focusing on the research progress.**



#### 3.1. Theoretical review

The main goal in this section is to replace the old OWC formulation for a new one, this last based on a real gas model, instead of the adiabatic process on an ideal gas. First of all, the classic problem will be analysed. Afterwards, the real gas model will be introduced and applied to the theoretical model.

##### a. OWC model review. Classic formulation

In the classic problem, Sarmiento (1990) and Martins-Rivas & Mei (2009) measured the outer (thermodynamic) pressure in the chamber with a manometer, and they supposed that its value is constant. Nevertheless, they considered that the external pressure is time-dependent under operating conditions. For this reason, a new problem is presented, see the sketch depicted in figure 2, where  $P_0$  and  $P_2$  are the outer reference thermodynamic pressure and the

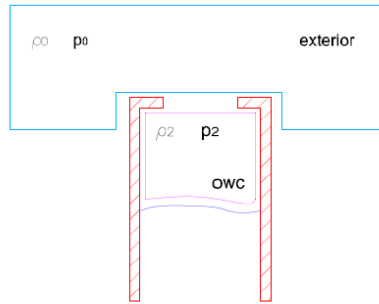
thermodynamic total pressure inside the chamber of the OWC, respectively. The difference of these pressures is the manometric pressure inside the chamber ( $p_{owc}$ ) as it is stated in the following equation:

$$P_2 = p_{owc} + P_0. \quad (1)$$

The continuity equation applied to the control volume is:

$$Q_T^m = -\frac{d}{dt}(\rho_2 V_{owc}) = -\left(\rho_2 \frac{dV_{owc}}{dt} + V_{owc} \frac{d\rho_2}{dt}\right), \quad (2)$$

**Figure 2: Control volume scheme.**



With the adiabatic relation,

$$pV^\gamma = \text{constant}, \quad (3)$$

and consequently

$$\frac{\rho}{\rho_{ref}} = \left[\frac{p}{p_{ref}}\right]^{1/\gamma}, \quad (4)$$

taking the solution ( $\rho_0, P_0$ ) as a reference, the linear relations between pressure and density are established in equation (1):

$$\rho_2 = \rho_0 + \left(\frac{\rho_0}{\gamma P_0}\right)(p_{owc}). \quad (5)$$

The mass flow that go through the turbine,  $Q_T^m$  is defined respect to the external reference density as:

$$Q_T^m = \rho_0 Q_T = \rho_0 \frac{KD_T}{N\rho_0} p_{owc}, \quad (6)$$

where  $K$  depends on turbine parameters, following (8),  $D_T$  is the turbine diameter and  $N$  is the turbine rotation velocity.

Substituting in equation (2), and multiplying by  $\rho_0$ ,  $Q_{owc}$  is cleared up:

$$Q_{owc} = \frac{KD_T}{N\rho_2} p_{owc} + \frac{V_{owc}}{C_s^2 \rho_2} \left(\frac{dp_{owc}}{dt}\right), \quad (7)$$

where  $C_s$  is the speed of sound in air.

The continuity reads:

$$Q_{owc} = \frac{KD_T}{N\rho_2} p_{owc}, \quad (8)$$

with  $Q_{owc}$  and  $p_{owc}$  defined as real quantities.

In the classic problem, the air flow inside the OWC depends linearly on the pressure difference.

### b. Real gas properties

In the classic OWC problem, air is considered as a perfect gas bounded to a compression/exhaust adiabatic process inside the chamber and through the turbine. A more complete description of the process consist of supposing that there exists a mix of dry air and water vapour inside the chamber, so the displaced fluid does not fit the ideal gas model. Some characteristics of the air–water vapour mixture are deduced from the properties of the vapour fraction. Using the Clapeyron-Clausius law (9), the saturation vapour pressure  $e_s$  is defined as:

$$e_s = e_0 \cdot \exp\left[\frac{L}{R_v} \left(\frac{1}{T_0} - \frac{1}{T}\right)\right], \quad (9)$$

where  $e_0 = 0.611 \text{ kPa}$  is the partial saturation pressure at  $T_0 = 273 \text{ K}$ ;  $L$  is the latent vaporisation heat;  $R_v = 461 \text{ J/K.kg}$  is the water vapour constant, and  $L/R_v = 5423 \text{ K}$ .

However, the vapour pressure at any temperature —any non–equilibrium state— is determined from a given value of relative humidity ( $RH$ ), expressed as the vapour concentration in dry air referred to the vapour concentration at equilibrium:

$$RH = \frac{e}{e_s}, \quad (10)$$

The real gas density is corrected from the dry air density using the mixing ratio  $r$ , defined as the ratio between the masses of vapour and dry air

$$r = \frac{m_v}{m_a} = \frac{\epsilon e}{p}, \quad (11)$$

where  $\epsilon = \frac{R_a}{R_v} = \frac{28607}{461} = 0.622$ . The moist air density is expressed as:

$$\rho_m = \rho_a \frac{1+r}{1+r/\epsilon} = \rho_a \frac{1+r}{1+1.608r}. \quad (12)$$

### c. Real gas model for the OWC

We start from the equation of state for  $N$  mols of an ideal gas:

$$pV = NR_0T, \quad (13)$$

The real gas is expected to deviate from the ideal law, with the appearance of several interactions between different thermodynamic variables. To deal with the real gas, we start defining the compressibility factor per gas mole,  $\mathbb{Z}$ , (Biel Gayé, 1986), (Prausnitz, 1999), as:

$$\mathbb{Z} = \frac{pV}{R_0T}, \quad (14)$$

where  $R_0$  is the universal gas constant. For an ideal gas,  $\mathbb{Z} = 1$ .

The specific heat and the enthalpy for the real gas, as deviations from the ideal gas values, (Yang & Su, 2004):

$$C_{pg} = C_p + \delta C_p p, \quad (15)$$

and:

$$H_g = H + \delta H p, \quad (16)$$

where the deviations of specific heat and enthalpy are:

$$\delta C_p = -\frac{R_g T_r}{p_c} \frac{d^2}{dT_r^2} (f_0 + \chi_{mol} f_2) , \quad (17)$$

and:

$$\delta H = \frac{R_g T_c}{p_c} (f_0 + \chi_{mol} f_2) - T_r \frac{d}{dT_r} (f_0 + \chi_{mol} f_2) . \quad (18)$$

Following the methodology proposed by Yang & Su (2004) in a simplified way and making use of equations (15) to (18), the conservation of enthalpy is applied between turbine inlet and outlet, with known values of local temperature, pressure and humidity at the inlet. Recalling that the enthalpy for the ideal gas is expressed as:

$$H = C_p T + \frac{1}{2} U^2 , \quad (19)$$

The velocity at the turbine outlet is computed from equations (15) and (19) for the real gas:

$$U_{out} = \sqrt{2(H_g - C_p T_{out} - \delta H p_{out})} , \quad (20)$$

Here the temperature  $T_{out}$  should not be evaluated through the adiabatic process equation  $T_{out}^{ad} = T_{in} (p_{out}/p_{in})^{(\gamma-1/\gamma)}$ , because strictly speaking this last expression is only valid for ideal gas. Instead of using this last equation, a new value of  $T_{out} \neq T_{out}^{ad}$  is supposed until the continuity condition is satisfied:

$$\rho_g U S_{in} = \rho_g U S_{out} . \quad (21)$$

The iterative procedure, in which the effect of moisture is implemented through the density and the real gas constant  $\rho_g$ , outcomes new pressure and temperature values for the real gas. Applying this methodology, we will observe differences between the ideal and real gas models.

#### d. Turbine dynamics

The OWC uses a power take off system for transformation of pneumatic energy into electricity to be supplied to the grid. Usually, it uses a turbine to accomplish with that purpose.

The primary input for the design of a turbine is the pneumatic power based upon the pressure amplitude (P) and the volume flow rate Q at turbine inlet. The performance indicators are the pressure drop, power and efficiency, and their variation with the flow rate. The aerodynamic design and consequent performance is a function of several variables that have been listed by Raghunathan (1995).

In general terms, the turbine performance is described by the following non-dimensional coefficients:

- Flow coefficient:  $\Phi = \frac{V_x}{U} , \quad (22)$

- Pressure drop:  $P^* = \frac{\Delta P}{\rho_2 \omega^2 D_t^2} , \quad (23)$

- Solidity:  $\sigma = \frac{A_a}{\pi (\frac{D_t}{2})^2} , \quad (24)$

where  $V_x$  is the axial velocity,  $U = ND_t/2$  is the blade circumferential velocity,  $\omega$  is the relative incoming velocity,  $A_a$  is the whole blades area.

The non dimensional power input is expressed as:

$$W^* = P^* \cdot \Phi \quad (25)$$

### 3.2. Experimental set up

We describe in this section the methodology used to conduct tests in a wind tunnel. The turbine performance has been tested with a total of three different environmental conditions: so called "dry air" (non-forced humidity, environmental conditions, 35% relative humidity), humid air with minimum humidity (50% relative humidity) and humid air with maximum humidity (70% relative humidity).

#### a. Wind tunnel

The wind tunnel is a poly-methylmethacrylate (PMMA) structure with a test section that is 3m in length with a 360mm x 430mm cross-section. The wind speed, up to 20m/s, is controlled by a variable frequency converter controlling an electric fan at the downstream end with a maximum power of 2.2 kW.

First of all, the wind tunnel calibration was made. This tunnel is controlled by an inverter *Siemens Micromaster 420*. An input voltage is introduced to the inverter, and this transforms it to a valid voltage for the wind tunnel engine. With the calibration, it is desirable to know the relation between input voltage and wind velocity.

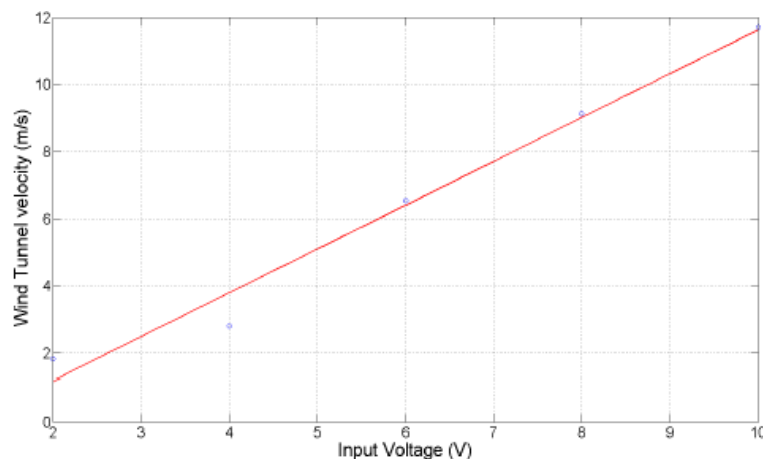
The calibration has been made in dry tests, so the measure is not affected by humidity. The measure was done with a Prandtl tube. This takes total ( $P_T$ ) and static ( $P_S$ ) pressure data, and with these, it is calculated the velocity as:

$$v = \sqrt{\frac{2(P_T - P_S)}{\rho}} \quad (26)$$

where  $\rho$  is the fluid density.

The calibration curve obtained is depicted in figure 3, finding a linear response with the input voltage, with a linear regression coefficient  $R = 0.9979$ . The maximum input voltage, 10V, is equivalent to a wind velocity of 11.7m/s for the used configuration in the inverter.

**Figure 3: Wind tunnel calibration.**



#### b. Turbine

It has been used a turbine of diameter  $D_t = 0.025m$ .

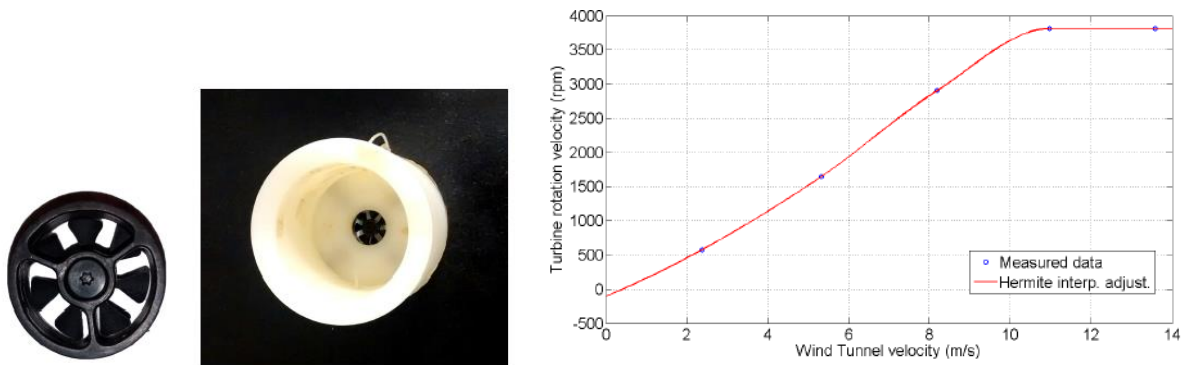
The turbine frontal area is  $A_t = 3.5906 \cdot 10^{-4} m^2$ , and the turbine blades area is  $A_a = 2.4271 \cdot 10^{-4} m^2$ . The turbine solidity, required for equation (24), has a constant value of  $s = 0.3434$ .

This turbine, shown in figure 4, has been assembled on a nylon structure which simulates an OWC (see figure 4).

### Turbine calibration

The rotation velocity of the used turbine was calibrated. As shown in figure 4, the relation between rotation speed and wind tunnel air velocity is linear until the turbine reaches its terminal velocity.

**Figure 4: Image of the turbine and the nylon structure, and turbine calibration.**

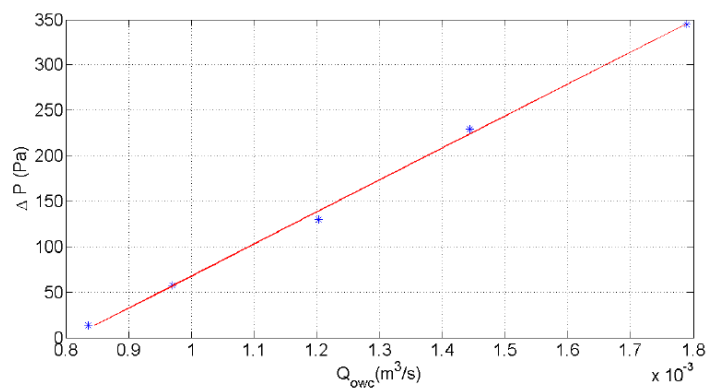


### c. Experimental model scope and restrictions

The turbine is not a Wells turbine strictly speaking, so the one used in this study does not rotate in the same direction independently of the air flow, as the real Wells turbine does.

These two turbines have the same behaviour, as the relation between air flow and pressure is linear, see figure 5.

**Figure 5: Air flow and pressure drop in turbine.**



This fact allows focusing on the humidity change and its effect in flow and turbine rotation. Additionally, in these tests there is an important fact to be considered: the forced environmental conditions inside wind tunnel (humidity and temperature) are unique. The repeatability of the experiments is almost null, as the moist measurement depends on a high number of other

factors: external temperature, time of the day, season and wind tunnel location. There is a high level of humidity in the laboratory, so it is a really influencing condition on wind tunnel moisture.

#### d. Water spray gun

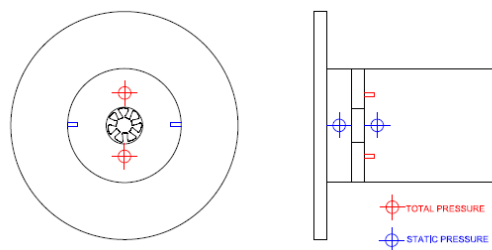
A paint spray gun is used with water to seed the wind tunnel with small water particles. The gun is situated in front of the wind tunnel entrance, so the engine in the other end of the tunnel sucks the air and water particles out, generating and humid air circulation. The nozzle aperture is controlled with a faucet in the bottom of the gun. In the measurements presented in this work, the maximum and the minimum apertures have been tested to allow us maximum and minimum humidity conditions inside the tunnel, respectively.

#### e. Measurement instruments

##### Pressure

The pressure measurements have been conducted with the pressure system *DTC Initium* by *Measurement Specialties INC*. It consists of a number of pressure taps (up to 64 channels per scanner). These work at a sampling period of 0.0016 s. Six pressure taps have been located around the turbine: two of them in the flow direction to measure total pressure, and the rest four samples perpendicular to the flow direction, for the static pressure measurement (see figure 6). There are two static pressure taps and two total pressure taps place upstream the turbine, and two static pressure taps placed downstream.

**Figure 6: Pressure taps distribution.**



##### Air flow velocity

The wind velocity has been measured with a *Laser Doppler Velocimeter (LDV)* by *TSI*. This is an extremely precise technique, and as a seeding, it is used the water particles in the wind tunnel. Hence it is obtained a complete velocity profile in every point needed. In this case, it has been measured the velocity upstream and downstream turbine.

##### Turbine rotation

The turbine rotation has been measured with a *Laser Distance Measurement Device Selcom SLS5000*. The main objective of this device is measuring distances. Thus, every time a blade passes through the laser, its signal changes. Obviously, if the blade remains at the same distance, the laser gives an identical signal for every single blade of the turbine. With a spectral analysis of the signal, the average rotation frequency is obtained.

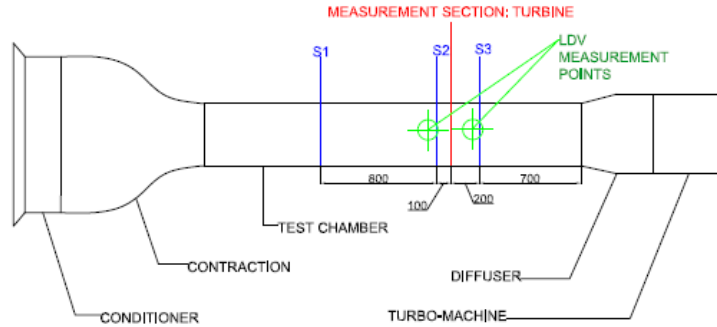
##### Humidity and temperature

The measurement of humidity and temperature has been done with a weather station *Oregon Scientific BAR908HG*. This can support a maximum of five thermo-hygrometer remote sensors. In this case, it have been used three remote sensors, using in addition the sensor inside the station to measure the external temperature and humidity. The three remote sensors were located at three representative sections inside the wind tunnel (S1, S2 and S3), as shown in figure 8. The first one is placed near the entrance to control the input humidity. The second one is situated upstream the turbine, near it, and the third one, downstream.

**Figure 7: Wind tunnel.**



**Figure 8: Final set up.**



At first instance, some equilibrium humidity tests were performed to analyse how humidity changes with time. In the final tests and in order to obtain accurate results, it was required experimentally to have a humidity level as constant as possible.

The final set up, with the thermo-hygrometer sensors and the *LDV* measurement points is shown in figure 8.

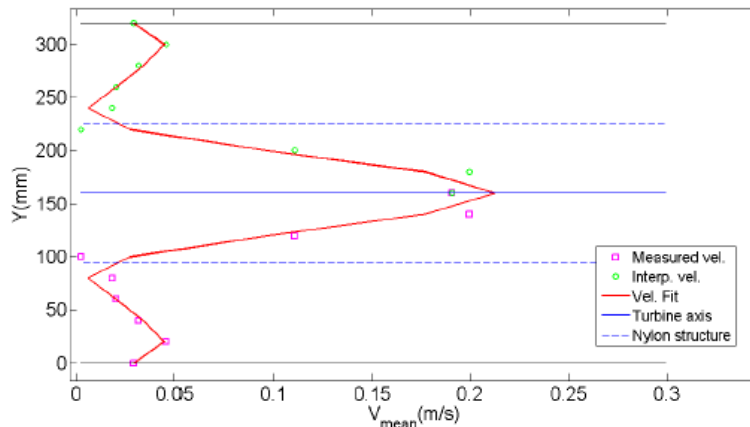
## 4. RESULTS

In this section, experimental results are presented alongside the theoretical prediction through the real gas model shown in previous sections.

### 4.1. Upstream velocity profile

In the experimental set up, the OWC nylon structure pit is an obstacle to the air flow, enhancing the formation of stagnation points in the edges of the structure. To quantify this aspect, some velocity measurements have been carried out by using *LDV* in the inlet region of the structure.

**Figure 9: Velocity profile. LDV. Turbine inlet.**

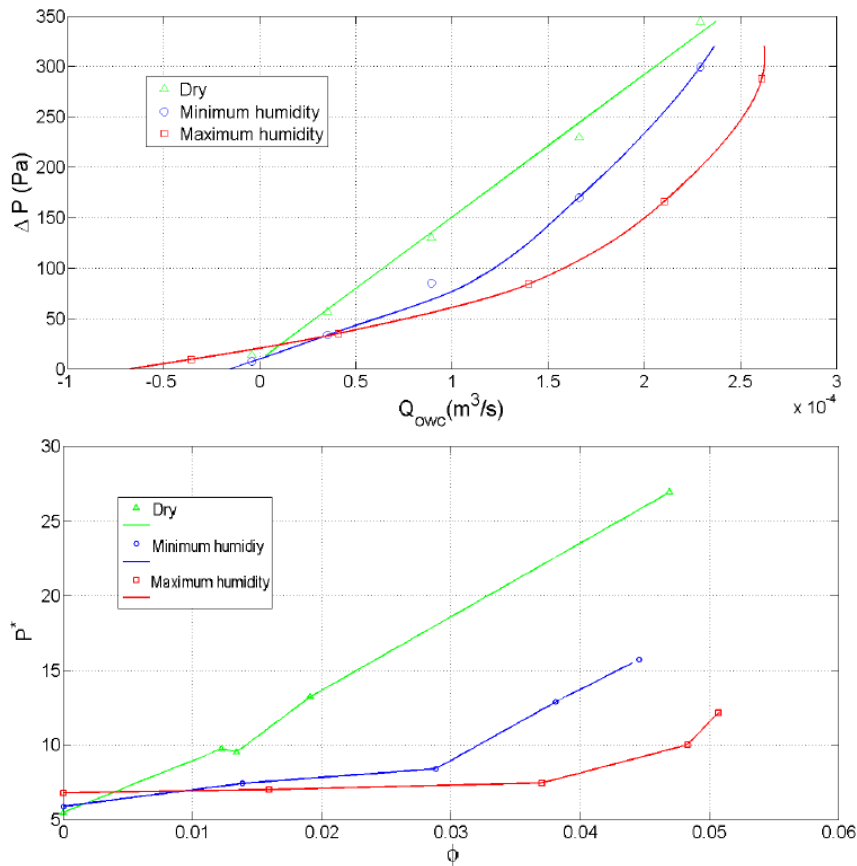


The velocity profile grows around the turbine orifice, with a minimum in the intersection with the nylon structure. The values are lower than in the downstream because of the energy conservation: a decrease in pressure implies an increase in velocity.

#### 4.2. Pressure drop and air flow

The pressure difference between upstream and downstream was measured for every test. It is shown in figure 10 that the pressure—flow rate curves for humid air present a different behaviour in comparison to the dry air one. In addition, as humidity increases, the curve moves away from the dry air one. In other words, it is necessary greater flow rates to obtain the same pressure drop as humidity increases. Consequently, humid air brings less power to the turbine, as shown in following sections.

**Figure 10: Pressure drop and air flow. Dimensional (up) and non-dimensional (down).**



#### 4.3. Non-dimensional pressure drop and air flow

As presented in equations (22) and (23), in the classic turbines literature, the turbine performance is described by some non-dimensional coefficients. In our case, a representation of the pressure drop and the air flow in terms of non-dimensional coefficients is useful for later comparison with future tests.

The results are depicted in figure 10. Dry air curve exists in a different non-dimensional pressure range than the humidity cases. For  $\phi \geq 0.02$ , when the flow starts to be significant, and non-linear effects are neglected, the curves with humidity start to diverge with respect to the air flow. The behaviour of dry air curve with respect to the other two humidity curves is different. For the two humidity curves, the pressure range is the same. As well as in the

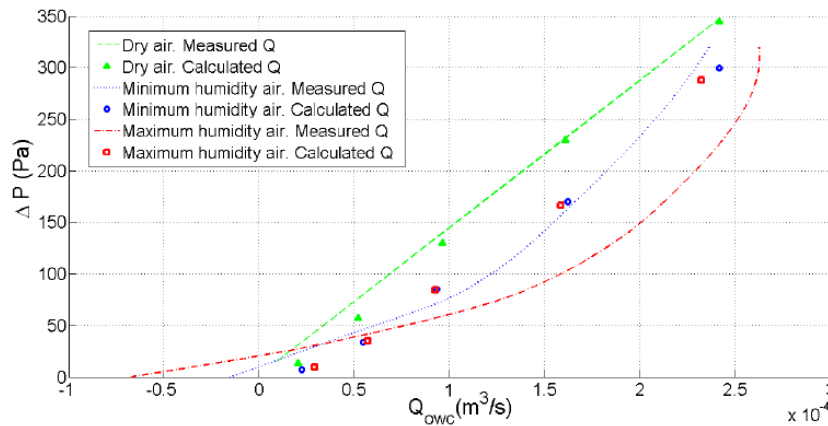
dimensional case, with greater humidity, to obtain the same pressure a higher flow coefficient is necessary.

#### 4.4. Density correction by the air–vapour mixture

We have seen in previous sections that the form of the curves  $\Delta P-Q$  is different depending on the humidity content of the air flow. A first attempt in predicting the turbine response under moist air condition, is performed by substituting moist air densities calculated by equation (12) in the classic continuity equation (8). But in this case, the classic formulation does not allow to predict successfully the turbine response under moist condition, as depicted in figure 11.

The turbine response for dry conditions is fairly well predicted with the classic formulation. However, the moist conditions do not match the experimental results. That way, the classic continuity expression might result incomplete for the prediction of the turbine performance with humid air, even if the actual turbine also offers a linear response in dry air.

**Figure 11: New humidity curves. Corrected density.**

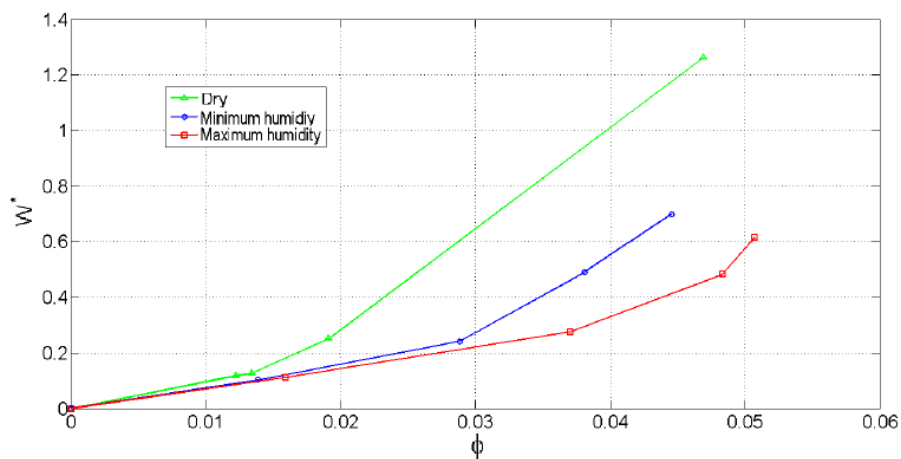


#### 4.5. Power input

Power input is calculated as shown in equation (23). The results obtained are presented in figure 12.

Following the same argument of previous results, the power input decreases as humidity increases, for a constant flow rate. In other words, to obtain the same power input it is necessary greater flow rates with greater values of humidity.

**Figure 12: Non dimensional power input and air flow.**



## 5. CONCLUSIONS

Throughout the development of this work it has been shown the behaviour of moist air on the operation of an air turbine. In particular, the results presented after the application of the theoretical model of real gas are intended to be further applied to improve the performance of OWC devices.

The relation between pressure drop and air flow in classic theory is linear, and the hypothesis of dry air and ideal gas are assumed. With these experimental tests it has been observed that this relation is not linear with moist air. Furthermore, it has been justified for the air–water vapour mixture, that linear curve decreases towards the experimentally observed values when moisture exists.

It has been found that the flow through the turbine does not address the ideal gas law, hence the adiabatic equation for the ideal gas is not fully applicable. For the conservation of mass flow and enthalpy to be fulfilled, a real gas model has to be applied. In that sense, it has been verified that the real gas temperature output differs from the ideal gas adiabatic prediction. Moreover, as humidity increases the difference between adiabatic temperature and flow conservation temperature grows. The compressibility factor is close to 1, but does not take exactly that value. The real gas differs slightly from the ideal model. The state equation for the real gas differs from the ideal case, and therefore its behaviour keeps away from the ideal adiabatic description of the process.

It has been found that power input decreases when moisture increases. The difference between expected power output values and real power obtained in operating OWC plants may be revised under these considerations.

## REFERENCES

- Biel Gayé, J. (1986). *Formalismo y método de la termodinámica. Teoría general, aplicaciones y ejercicios resueltos. Apuntes de clase*. Universidad de Granada.
- Evans, D. (1982). Wave-power absorption by systems of oscillating surface pressure distributions. *Journal of Fluid Mechanics*, 114, 481–499.
- Evans, D. & Porter, R. (1995). Hydrodynamic characteristics of an oscillating water column device. *Applied Ocean Research*, 17, 155–164.
- Martins-Rivas, H. & Mei, C. (2009). Wave power extraction from an oscillating water column at the tip of a breakwater. *J. Fluid Mechanics*, 626, 395–414.
- Power-technology (2014). Internet article, available at: <http://www.power-technology.com/projects/mutriku-wave/>.
- Prausnitz, J., Lichtenthaler, R., & de Azevedo, E. G. (1999). *Molecular Thermo-Dynamics of Fluid-Phase Equilibria*. Prentice–Hall.
- Raghunathan, S. (1995). The wells air turbine for wave energy conversion. *Prog. Aerospace Sci.*, 31, 335–386.
- Sarmiento, A., Gato, L., & Falcao, A. (1990). Turbine-controlled wave energy absorption by oscillating water column devices. *Ocean Engineering*, 17(5), 481–497.
- Singh, S. & Kumar, R. (2012). Ambient air temperature effect on power plant performance. *International Journal of Engineering Science and Technology (IJEST)*, 4(8), 3916–3923.
- Tsonopoulos, C. & Heidman, J. (1990). From the virial to the cubic equation of state. *Fluid Phase Equilibria*, 57, 261–276.
- Yang, W. & Su, M. (2004). Influence of moist combustion gas on performance of a sub-critical turbine. *Energy Conversion & Management*, 46, 821–832.

